Yoonsun Yang[1]
Séverine Le Gac[2]
Leon WMM Terstappen[1]
Hoon Suk Rho[2]

[1]Medical Cell BioPhysics Group, MIRA Institute for Biomedical Technology and Technical Medicine, University of Twente, The Netherlands
[2]Applied Microfluidics for BioEngineering Research Group, MESA+ Institute for Nanotechnology, MIRA Institute for Biomedical Engineering and Technical Medicine, University of Twente, The Netherlands

Received September 5, 2017
Revised November 7, 2017
Accepted November 20, 2017

Research Article

Parallel probing of drug uptake of single cancer cells on a microfluidic device

Drug resistance is frequently developing during treatment of cancer patients. Intracellular drug uptake is one of the important characteristics to understand mechanism of drug resistance. However, the heterogeneity of cancer cells requires the investigation of drug uptake at the single cell level. Here, we developed a microfluidic device for parallel probing of drug uptake. We combined a v-type valve and peristaltic pumping to select individual cells from a pool of prostate cancer cells (PC3) and place them successively in separate cell chambers in which they were exposed to the drug. Six different concentrations of doxorubicin, a naturally fluorescent anti-cancer drug, were created in loop-shaped reactors and exposed to the cell in closed 2 nL volume chambers. Monitoring every single cell over time in 18 parallel chambers revealed increased intracellular fluorescence intensity according to the dose of doxorubicin, as well as nuclear localization of the fluorescent drug after 2 h of incubation. The herein proposed technology demonstrated a first series of proof of concept experiments and it shows high potential to use for probing drug sensitivity of single cancer cell.

Keywords:
Drug uptake / Microfluidics / Single cell analysis DOI 10.1002/elps.201700351

Additional supporting information may be found in the online version of this article at the publisher's web-site

1 Introduction

Cancer cell responses to drugs vary greatly due to their genetic and phenotypic heterogeneity [1, 2]. Investigation of cancer cell response to drugs is mostly performed on cell populations resulting in an average value for the cell population while masking the information on small subsets of cells. For example, during tumor progression, a small sub population of tumor cells often becomes resistant to the drug, which can easily missed when the cell population is investigated as a whole [3]. Therefore, characterizing the response of individual cells to drugs is urgently needed as not to miss any information on the possible acquired resistance to the treatment of certain cells in the tumor.

Drug uptake and accumulation is one of the important characteristics which directly correlates with drug efficacy [4]. Anthracyclines such as doxorubicin are attractive drugs for such studies, since their uptake can be monitored thanks to their intrinsic fluorescence. Thereby, this class of drugs can reveal differences in drug accumulation and distribution inside the cells that relate to the sensitive and resistance of the cells to this drug [5–7]. One of the conventional methods to isolate and probe single cells is based on flow cytometry after drug treatment [4]. However, this method precludes monitoring of the same cell over time. Monitoring cells in the bulk over time has been performed by fluorescence microscopy in well plates or cover slides [7, 8]. However, using this approach, it is challenging to monitor the same individual cell in the whole population and to isolate single cells in a well plate. The challenge is even larger when cells of interests are relatively rare such as stem cells or circulating tumor cells (CTCs). In addition, the volumes in traditional well plates of a few hundred microliters per well are relatively large for single cell studies.

Microfluidic devices have been used for drug screening analysis and reported advantages to conventional methods are the ability to manipulate cells, precise fluidic control, gradient generation of the drug, reduction of reagent volume and parallelization [9–12]. Especially, on-chip 2D or 3D cultures of cells were intensively investigated to mimic cellular tissues [9, 13–16]. Various concentrations of drug dose and combination of drugs combined with viability tests

Correspondence: Dr. Hoon Suk Rho, Applied Microfluidics for BioEngineering Research, University of Twente, 7500 AE Enschede, The Netherlands
E-mail: h.s.rho@utwente.nl

Colour Online: See the article online to view Figs. 1–5 in colour.

were presented [11, 16]. Droplet microfluidic technologies brought the capability of single cell high-throughput drug screenings [12,17–19]. Droplets encapsulating single cell with precisely dosed drug were incubated for a few days. Compartmentalized droplet in picoliters to nanoliters volume was used for the single cell drug test without any cross-contamination of other cells and reagents and viability test was performed in the drop. However, without arraying droplets, it is still challenging to monitor the same cell over time on the same chip. A recent study integrated droplet arrays to monitor drug accumulation in droplets and successfully showed long term monitoring of the same cells in the droplets [20].

A same single cell analysis device (SACSA) was developed to monitor the intracellular fluorescence intensity after exposure to drugs in a simple channel equipped with one capture structure by Li et al [21, 22]. This device allowed real time monitoring of the same single cell over time, but the first cell captured was monitored in continuous flow of drug solution therefore parallelization and various treatment conditions were not applied in this device. High-throughput microfluidic devices for monitoring the cellular response to stimuli both at the cell population level and single cell level over time has been demonstrated by different groups [11, 13, 23–29]. However, cells were again loaded in the device without any sorting step, so that a higher number of reactors had to be monitored than the number of cells of interest, which costs time and effort.

Recently, we developed a v-type valve for single particle and cell isolation [30]. This flexible valve can capture cells, identify the type of cells, and either isolate or discard it based on the microscopic observation. Here, we take advantage of this technology to pre-select individual cells and load them in 18 separate chambers, where we monitor drug uptake at the single cell level, using six different drug concentrations. Specifically, we report (i) the capture of individual cells in independent chambers using a v-type valve and flow manipulation by peristaltic pumping to introduce the cells in separate chambers, (ii) the generation of a series of different drug concentrations using 6 different reactors (loop-shaped reactors) and (iii) monitoring of drug uptake at the single cell level in 18 compartmentalized chambers with 2 nL volume. The device is characterized and validated first using beads and dyes. Altogether, this device shows great potential to increase our understanding of drug resistant phenotypes at the single cell level.

2 Materials and methods

2.1 Chip fabrication and preparation

Microfluidic devices were fabricated using polydimethylsiloxane (PDMS) multilayer softlithography [31] and we followed the protocols used in our previous studies [32, 33]. After the final adhesion step, the device was autoclaved for 20 min at 120°C for sterilization. To prevent non-specific binding of biomolecules, cell loading and pushing channels including cell chambers were treated with Pluronic® F-108 4% (Sigma-Aldrich Chemie N.V., Zwijndrecht, The Netherlands) for 5 min before use and washed for 1 min and filled with CO_2 independent culture medium (Gibco, Paisley, UK) including 10% Fetal Bovine Serum (FBS) and 1% Penicillin/Streptomycin (Pen/Strep).

2.2 Data acquisition

A stereomicroscope (Motic SMZ168, Lab Agency Benelux B.V., Dordrecht, The Netherlands) equipped with a CMOS camera (Moticam 3.0) was used to characterize peristaltic mixing in the device. To monitor fluorescent intensities of the fluorescent probe resorufin in the gradient generator unit, an inverted fluorescent microscope (Leica DMI 5000M, Leica Microsystems B.V., Son, The Netherlands) equipped with an automatic XY-stage (Oasis PCI XY control unit), and a digital camera (Leica DFC300 FX, Leica Microsystems B.V., Son, The Netherlands) was used. For acquisition of images of drug uptake by the cells an inverted fluorescent microscope (Olympus IX73, Olympus Netherlands B.V., Leiderdorp, The Netherlands) equipped with an automatic XY-stage (99S000, Ludl Electrnic Products Ltd., NY, USA), and a digital camera (ORCA-ER, Hamamatsu Photonics Deutschland GmbH, Herrsching, Germany) was used.

2.3 Reagent preparation for chip validation

One hundred micromolars of resorufin (Sigma-Aldrich Chemie N.V., Zwijndrecht, The Netherlands) solution was introduced into the drug solution inlet while the cell medium inlet for cell medium was filled used to introduce with Milli-Q water. After mixing the solutions in six independent reactors (Fig. 1C) for 2 min, fluorescent images were acquired for the 6 reactors using a Leica I3 filter cube (excitation: BP 450–490 nm; emission: LP 515 nm). Source 15Q (∅ 15 μm particles based on rigid polystyrene /divinyl benzene polymer matrix, GE Healthcare Europe GmbH, Eindhoven, The Netherlands) to be used as a surrogate for cells, were diluted to a 1:1000 ratio in Milli-Q water (500 000 beads/mL) for testing the particle capture and isolation in individual incubation chambers.

2.4 Cell culture and preparation

PC3 cells were cultured in RPMI-1640 media supplemented with 10% FBS and 1% Pen/Strep (all purchased from Sigma-Aldrich, Sigma-Aldrich Chemie N.V., Zwijndrecht, The Netherlands) at 37°C in 5% CO_2 atmosphere. After detachment of the cells using 0.05% of Trypsin/EDTA (Gibco, Paisley, UK), 500 000 cells were resuspended in 1 mL of CO_2 independent medium including 10% FBS and 1% Pen/Strep.

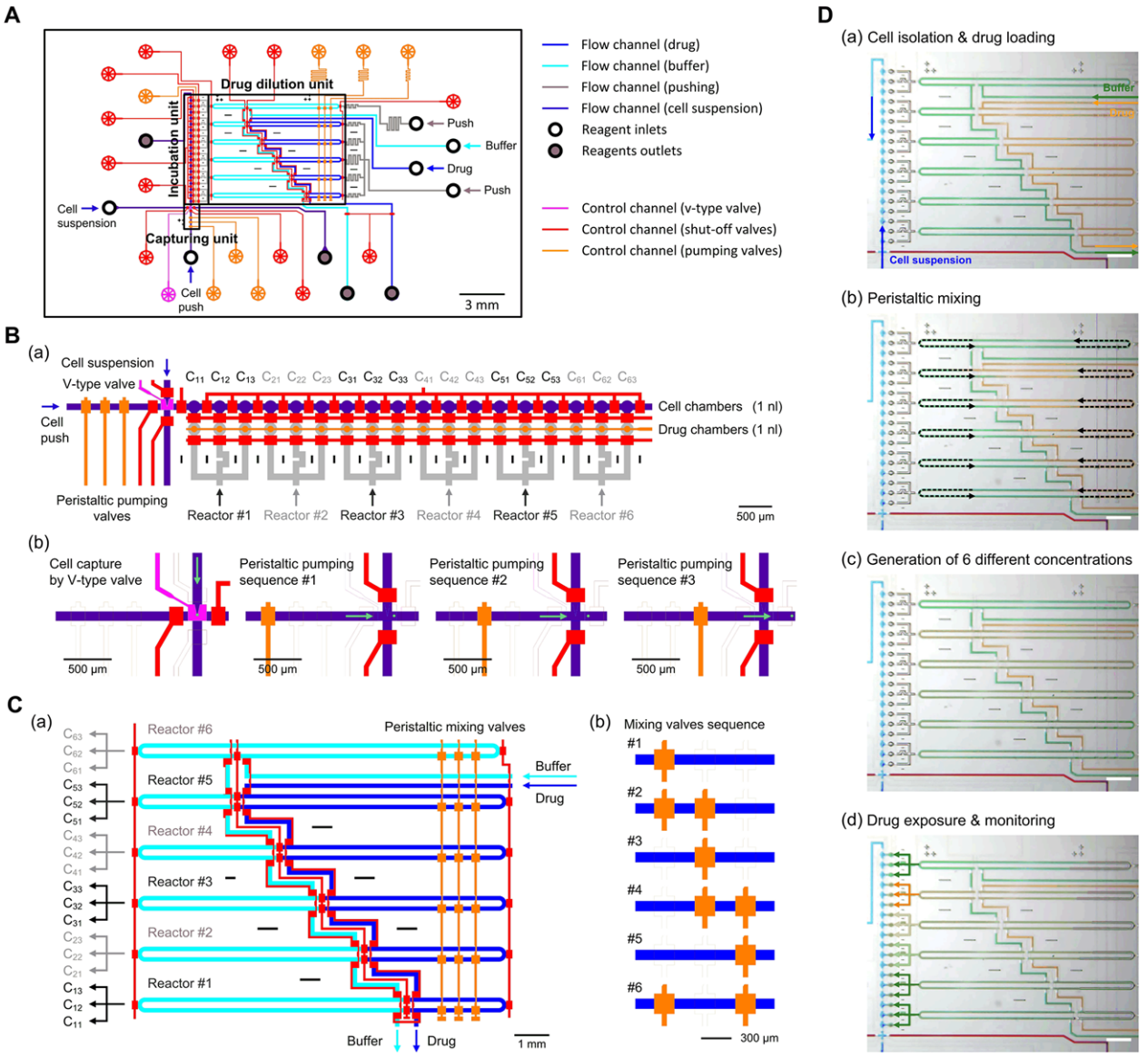

Figure 1. Design and operation of the microfluidic device. (A) AutoCAD design of the entire device. (B) (a) magnified image of the incubation chambers and capture unit. (b) Schematic view of the single cell capture and isolation using a v-type valve and peristaltic pumping. (C) Series of 6 reactors. (D) Operation procedure of the microfluidic device. (a) Single cell isolation, drug and medium loading into the channels. (b) Mixing solutions in the reactors in the drug dilution unit using operating micro-valves. (c) Creation of six different concentrations after mixing. (d) Various doses of drugs exposed to the cells in the incubation chambers (1 mm scale bars are shown).

2.5 Drug exposure experiment

A total of 10 mg of doxorubicin hydrochloride (Sigma-Aldrich, Sigma-Aldrich Chemie N.V., Zwijndrecht, The Netherlands) was dissolved in 1 mL of Milli-Q water and diluted in CO_2 independent medium to yield a 100 μM solution (58.8 μg/mL). After drug loading and on-chip cell exposure, the device was incubated on an AmpliSpeed slide cycler (Advalytix AG, Munich, Germany) at 37°C and images were acquired after 1, 2, and 4 h for all independent exposure chambers using a Olympus U-FGNA filter (excitation: BP 540–550 nm; emission: LP 575–625 nm). Values for fluorescence intensities were obtained after subtraction of the background value.

3 Results and discussion

3.1 Device design

The microfluidic device consists of a cell capture unit, an incubation unit, and a drug dilution unit as shown in Fig. 1A The incubation unit consists of 18 incubation chambers and each incubation chamber includes one cell chamber and one drug chamber (Fig. 1B (a)). A v-type valve, as recently reported by us [30], is incorporated to select and capture individual cells, which are subsequently placed into the individual cell chambers by peristaltic pumping with three valves (Fig. 1B (b)). A gradient generator unit consisting of 6 loop-shaped reactors

allows creating a series of six different drug concentrations. The drug and buffer solutions are loaded into the drug sites and buffer sites into the reactors through dedicated inlets (Fig. 1C). The volumes of drug sites in reactors 1, 2, 3, 4, 5 and 6 are 10.5, 15.5, 20.5, 25.5, 30.5, and 0 nl and the volume of buffer sites in reactors 1, 2, 3, 4, 5, and 6 are 30.5, 25.5, 20.5, 15.5, 10.5, and 41 nl, respectively. Consequently, the dilution rates of drug solution from reactor 1 to reactor 6 after dilution are 0, 0.26, 0.38, 0.50, 0.62, and 0.74 of stock solution (Detailed information is shown in Supplementary Table 1). Each reactor is connected to 3 drug chambers, allowing testing the six different drug concentrations in triplicates.

Figure 1D shows the operation procedure of the device. Here, the fluidic channels were filled with color dyes for visualization purposes. (Supporting Information Movie 1) First, cells are individually and successively captured by the v-type valve, and placed into the incubation chambers by peristaltic pumping (blue color lines). Thereafter, the drug stock solution (orange color lines) and cell culture medium (green color lines) are loaded through dedicated inlets in the drug and buffer sites, respectively, into the metering channels of reactors (Figure 1D (a)). During loading of the reagents, the metering valves are closed to separate the reactors into the drug site and the buffer site. Next, the side valves are closed and the metering valves opened to create six different closed loop-shaped mixers. Three micro-valves are actuated sequentially to enhance mixing of the reagents (Figure 1D (B)). Figure 1D (c) shows the resulting six different drug solutions with different concentrations prepared by the series of six reactors. Following this, the resulting drug solutions at different concentrations are introduced into the 18 drug chambers. Upon opening the valves between the cell and the drug chambers, the cells start to be exposed to various drug doses. (Figure 1D (d)).

3.2 Generation of a series of different drug concentrations using 6 reactors

For the creation of six different concentrations, the volume of drug solution and cell culture medium were metered and mixed in the channels of the reactor, as depicted in Fig. 1C. To enhance the mixing of the two reagents, the six reactors were equipped with three shut-off valves acting as a peristaltic pump [34]. The performance of the mixing valves was tested using a blue dye solution and Milli-Q water, introduced respectively into the channels designed for the drug solution and cell culture medium (Fig. 2A (a)). The three mixing valves in each reactor were operated in the following sequence to achieve peristaltic mixing: (1 0 0), (1 1 0), (0 1 0), (0 1 1), (0 0 1), and (1 0 1) where 1 represents a closed valve and 0 represents an opened valve [34]. The operating frequency of the sequence was changed from 1 to 30 Hz, and the mixing efficiency for these different conditions was evaluated in real-time. Figure 2A (b) shows pictures extracted from a time-lapse recording for one of the six reactors in which the two reagents were loaded in a 1:1 ratio. The mixing efficiency was evaluated by measuring over time the average brightness in a specific ROI (region of interest) by Image J software (Fig. 2A (c)). A parabolic profile of the blue fluid was generated, and lengthened in the channel over time upon sequential actuation of the mixing valves. Therefore, the interface between the blue dye and water became larger and assisted diffusion of the two solutions. The brightness value in the ROI was observed to fluctuate over time, while becoming smaller, and complete mixing was achieved when the average brightness of the ROI became constant, as illustrated in Fig. 2A (c). We observed that the mixing time decreased according to an increase of the actuation frequency below 19 Hz and increased slightly above 19 Hz. The optimal operating frequency was found to be approximately 19 Hz, and this condition was used in the other experiments for mixing of the two reagents.

To validate and quantify the generation of a series of six drug concentrations, we loaded 100 μM of resorufin solution into the channel for the drug solution and Milli-Q water into the channel for cell culture medium. We used resorufin as an alternative to doxorubicin, since the intrinsic fluorescence intensity of free doxorubicin is too weak to be visualized. Figure 2B (a) shows the volume ratio of Milli-Q water to the 100 μM of resorufin solution in the six reactors. After 1 min of mixing at 19 Hz, we acquired images in the six reactors by fluorescence microscopy and the mean fluorescence intensity was quantified in the same ROI as before using Image J software. Figure 2B (b) shows microscopy images taken in the six channels at a reactor after mixing was completed, and the measured corresponding intensities ($n = 3$). A linear relationship between calculated concentrations and the measured fluorescence intensities was obtained, as shown in Fig. 2B (b), and we successfully demonstrated the creation of six different drug concentrations in the device.

Following this step, the six different solutions were loaded into the 18 drug chambers, next to the cell chambers. After filling the drug chamber, the valve between the cell and the drug chambers were opened to let the drug solution diffuse into the cell chamber without any active mixing. To estimate diffusion time of the drug by real-time recording, a blue dye was loaded into the drug chamber while Milli-Q water was introduced in the cell chamber, and the brightness values in three ROIs in three different cell chambers were monitored over time (Fig. 3). Microscopy images of these three chambers at 0, 10, 60, and 300 s are shown in Fig. 3A. The value of the brightness in the cell chamber changed from 220, represented as white, to 180, represented as a blue color, within 300 s, as depicted in Fig. 3B. The brightness values of the three ROIs in the first 10 s are inserted in an inset in Fig. 3B to show the initial stage of the mixing.

3.3 Selection and capture of individual cells in independent chambers

A v-type valve is integrated in the microfluidic device at the beginning of the capture unit to isolate individual cells from a solution, as illustrated in Fig. 1B (b). We applied a pressure of

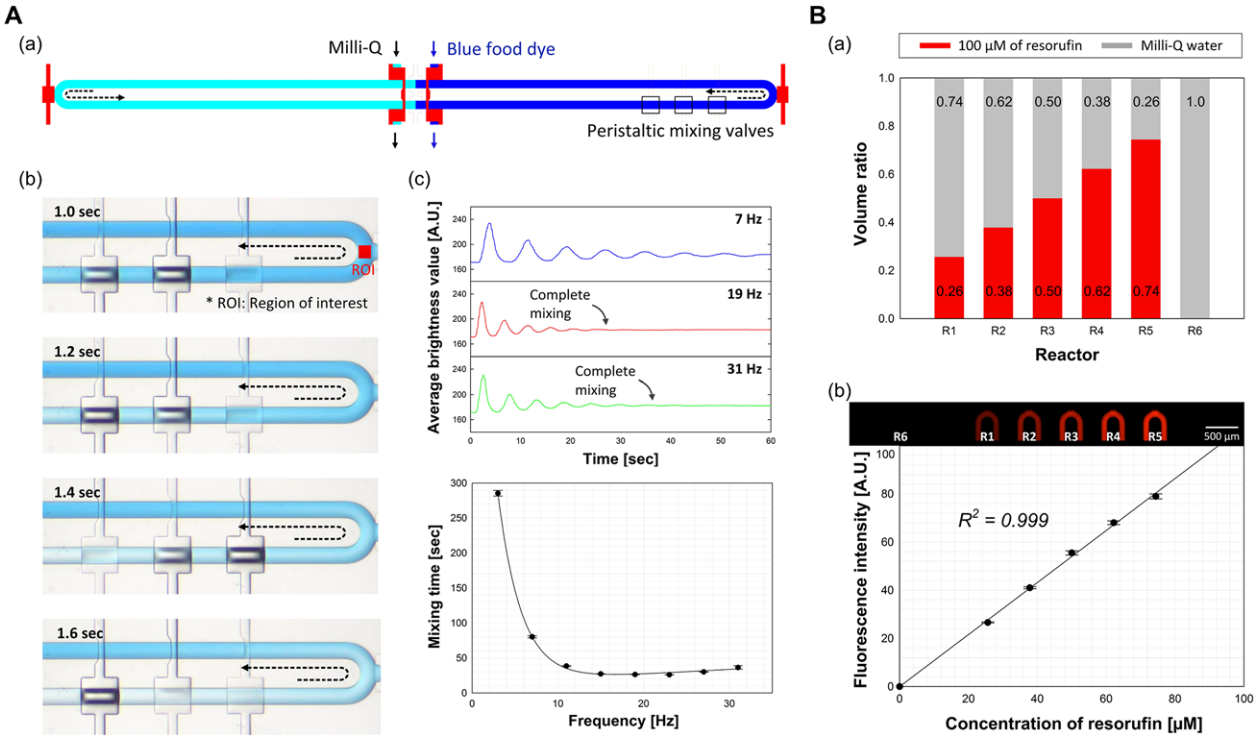

Figure 2. Validation of the drug dilution unit. (A) Peristaltic mixing in the reactors. The design of a reactor consisted of a drug site and a cell culture medium site. Two solutions (blue dye and Milli-Q water) were introduced in a 1:1 ratio into a reactor #4 (a). Time-lapse microscopy images of a portion of the channel were acquired during mixing at 19 Hz at different time points (b). Variations in the average brightness value in the ROI were measured as a function of time and the times for complete mixing were determined at various operating frequencies (c). (B) Generation of six different concentrations of resorufin. A non-linear concentration gradient of resorufin was obtained by loading Milli-Q water and 100 μM of resorufin solution in the six reactors (a). Resorufin fluorescence intensities were measured in the six reactors after mixing for 2 min at 19 Hz and plotted as a function of the calculated resorufin concentration ($n = 3$). At the top, microscopy images corresponding to the different concentrations are shown (b).

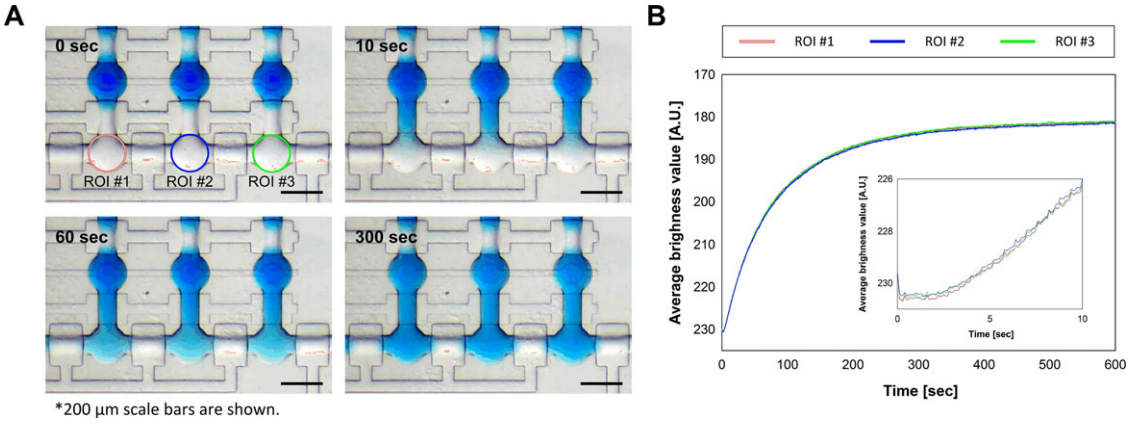

Figure 3. Estimation of the diffusion time in the incubation chamber. (A) Microscopy images of three chambers at 0, 10, 60, and 300 s after opening of the shut-off valve between the drug and cell chambers. The drug chambers were filled with blue color dye and cell chambers with Milli-Q water. (B) The value of average brightness in three cell chambers was monitored over time. In an inset, enlargement on the < 10 s zone of the graph is shown.

0.02 bar to load the cell suspension and 1.2 bar for actuating the v-type valve, as recently reported [30], for the capture of individual cells of interest, and this process was monitored through microscopy observation. In case multiple cells or cluster of cells were captured, we released the valve to let the cells flow into the outlet of the device without isolation. When a single cell was captured at the center of the v-type valve, the two shut-off valves located in the cell loading channels were closed and the shut-off valve in front of the incubation chambers opened. Subsequently, the captured cell was gently

moved into one cell chamber, using peristaltic pumping and three shut-off valves located on the pushing channels at the opposite side of the incubation chambers. These valves were actuated using the following sequence (0 0 1), (0 1 0), and (1 0 0), where 0 represents an opened valve and 1 represents a closed valve [35].

Cell capture and isolation was first evaluated using 15 μm diameter particles and cells of two different cell lines. Particles with a diameter of 15 μm were chosen as those have a uniform size which closely resembles that of cells. The v-type valve-based capture step was followed by an isolation step of the particle into the first chamber by peristaltic pumping. Then, the next particle was captured again by the v-type valve and pumped into the first chamber while the first particle was displaced into the next chamber. Using peristaltic pumping all particles were pushed into the cell chambers. To evaluate the distance of the movement of particles by the peristaltic pumping through the chambers we pumped the captured particle with Milli-Q water at various pumping frequency, from 1–3 Hz, for 2 s. The particle pumping test was repeated more than 100 times, and all particles moved into the first chamber after capture with a pumping frequency of 2 Hz. The particles, however, showed slightly different displacements which were dependent on the traveling length even under conditions in which the actuation time and speed were kept constant during pumping. As a consequence, not all individual cell chambers contain a single particle, and some chambers were empty or contained multiple particles as shown in Fig. 4A. Subsequently, we repeated this experiment using two different prostate cancer cell lines, LNCaP and PC3. The cell capture result in the 18 different cell chambers was not significantly different from the previous experiment with beads, as presented in Fig. 4B. Nine of the 18 chambers had a single particle or single cell while the rest of the chambers had either more than one cell or were empty. Figure 4C summarizes the number of cells isolated in 18 chambers after the capture and isolation of LNCaP and PC3 cells. In total, we performed four experiments in four independent devices, and 50% of chambers included single cells. The distribution of the number of occupied cells in each well does not follow a Poisson distribution [36] because the total number of cells in the cell chambers was determined by active control on the single cell capture process while the Poisson distribution applies to a passive process only governed by statistics.

To improve this single cell capture efficiency, we designed a 2nd generation device for future work as illustrated in Supplemental Figure S1. In this new design, shut-off valves placed between independent chambers are operated individually. Using this improved design, nine parallel chambers could be filled with individual cells in a reproducible manner.

3.4 Monitoring drug uptake in single cells

Intracellular drug accumulation is closely linked to drug efficacy. Furthermore, cell resistance property is often related to the transporting system to efflux drug. Therefore, characterization and monitoring of the drug uptake and its specific intracellular localization are important to understand mechanisms of drug resistance and determine drug efficacy. In a proof of concept experiment to demonstrate the suitability of our platform for such experiments, we isolated single PC3 cells in the 18 individual cell chambers and exposed them to various doses of the drug doxorubicin. Monitoring of drug uptake at single cell level was performed in 18 separate chambers. We used doxorubicin as a drug since it is intrinsically fluorescent, allowing thereby visualizing and monitoring the drug uptake by cells. Also, doxorubicin is localized mainly in the nucleus after cellular uptake, and its interaction with DNA is closely related to the drug sensitivity [7, 37]. Therefore, the doxorubicin fluorescence intensity was also evaluated in the nucleus and not only in the whole cell.

We introduced a 100 μM Doxorubicin solution into the metering channel and filled the other metering channel with CO_2 independent cell culture medium supplemented with 10% FBS and 1% Pen/Strep. Metering and mixing of the two reagents were performed as described earlier, for 2 min at 19 Hz in the closed reactors before they were introduced to the drug chambers. The number of cells in the cell chambers was shown in Fig. 4C (PC3 #2). Figure 5A presents images of the 18 independent chambers in one device after 2 h of incubation of the cells with doxorubicin. The final concentration of the drug in each incubation chamber ranges from 12.8 to 37 μM after the drug has diffused into the cell chambers, and is 0 μM for the control chambers (chambers C_{61} C_{62} and C_{63}) It is worth mentioning that the amount of drug loaded into the 1 nL volume drug chambers was as low as 15.1, 22.2, 29.4, 36.45, 43.5, and 58.8 pg for the different generated concentrations. To conduct the same experiment in a 96 well plate, 100 μL of 1 μM (0.58 μg/mL) to 10 μM (5.88 μg/mL) doxorubicin solution would be required, which is 1000–10 000 times larger than the amount of drug used here in one drug chamber.

We measured the doxorubicin fluorescence intensity in each individual cell, as presented in Fig. 5B, each bar corresponding to one individual cell. In case multiple cells were present in one chamber, they were numbered starting with the chamber number followed by 1, 2, and 3 for 3 cells; for example, $C_{52\text{-}1}$, $C_{52\text{-}2}$, and $C_{52\text{-}3}$. We observed that the doxorubicin intracellular fluorescence intensity increased according to the dose of doxorubicin introduced in the chambers, and no fluorescence was detected in the cells in the control chambers, (C_{61}, C_{62}, and C_{63}) which were only exposed to cell culture medium.

Next, we examined the localization of the drug in the cell. We set a ROI on the bright field image representing the whole cell area and one on the fluorescence image likely representing the position of the cell nucleus, as illustrated in the top left corner of Fig. 5C. It should be noted that pre-staining the nucleus with an intercalating dye would have been better to define the nucleus area, but this may have interfered with binding of doxorubicin since this drug is also a DNA

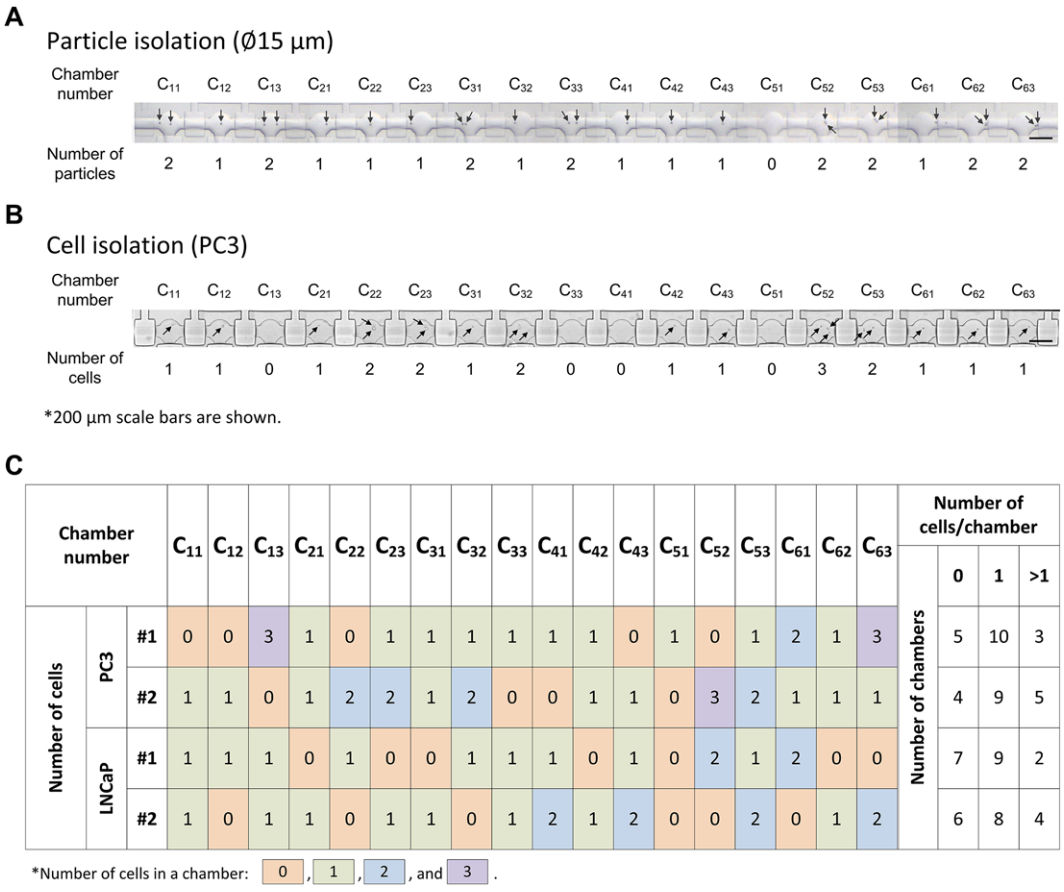

C

Chamber number			C11	C12	C13	C21	C22	C23	C31	C32	C33	C41	C42	C43	C51	C52	C53	C61	C62	C63	Number of cells/chamber		
																					0	1	>1
Number of cells	PC3	#1	0	0	3	1	0	1	1	1	1	1	1	0	1	0	1	2	1	3	5	10	3
		#2	1	1	0	1	2	2	1	2	0	0	1	1	0	3	2	1	1	1	4	9	5
	LNCaP	#1	1	1	1	0	1	0	0	1	1	1	0	1	0	2	1	2	0	0	7	9	2
		#2	1	0	1	1	0	1	1	0	1	2	1	2	0	0	2	0	1	2	6	8	4

Number of chambers

*Number of cells in a chamber: 0, 1, 2, and 3.

Figure 4. (A) Particle isolation in the cell chamber. (B) PC3 prostate cancer cell isolation in the cell chambers. Microscope images of isolated particles and cells in 18 incubation chambers in one device. (C) Summary of the cell capture in 18 cell chambers using prostate cancer cells, PC3 and LNCaP.

intercalating agent. For this reason, we did not include the result of 0 μM in Fig. 5C because without fluorescence signal we could hardly distinguish the nucleus from the cytoplasm. Figure 5C shows the fluorescence intensities of the area of the nucleus (black bar) and the cytoplasm (white bar) defined as subtraction of the fluorescence intensity of the nucleus of each cell from the total fluorescence intensity of the whole cell indicated by the bright field image. The ratio of the nuclear fluorescence to the whole cell fluorescence varied between 35 and 82% (mean 62%), without any clear relation with the drug amount.

It is feasible to monitor drug uptake over prolonged periods of time. We incubated single cells in a microfluidic device and images are acquired at 1, 2, and 4 h and drug uptake and localization was observed in most cells within 2 h. (Supporting Information Fig. 2) In future studies, the incubation chambers could be coated with collagen or fibronectin, and perfusion used over adherent cells for longer time monitoring, and cytotoxicity tests conducted in situ after cell exposure to the drugs. We demonstrated here the expose of individual cells to various drug doses and measured their drug uptake in our microfluidic device.

4 Concluding remarks

We developed a microfluidic device for probing drug uptake at the single cell level. Isolation of cells was performed using a v-type valve on the device followed by isolation in the incubation chambers using peristaltic pumping. Generation of various concentrations was successfully obtained using peristaltic mixing in the closed reactors and loaded into the precisely volume controlled chamber. Individual cells exposed to various drug doses were monitored for several hours. Intracellular fluorescence intensity was correlated with the drug dose and intracellular localization of the drug in the nucleus was clearly observed after 2 hr incubation already.

This proof of concept experiment showed the high potential of the device for probing drug uptake at the single cell level in a volume that is 1000–10 000 times reduced from traditional single cell analysis. The use of MDR (multidrug resistance) gene expressing cell lines could provide a nice model system to test changes in drug uptake over time for the future study. Treatment with potential inhibitors against the drug transporter (P-gp) could be used further demonstrate the potential of this technology to study drug response at the single cell level.

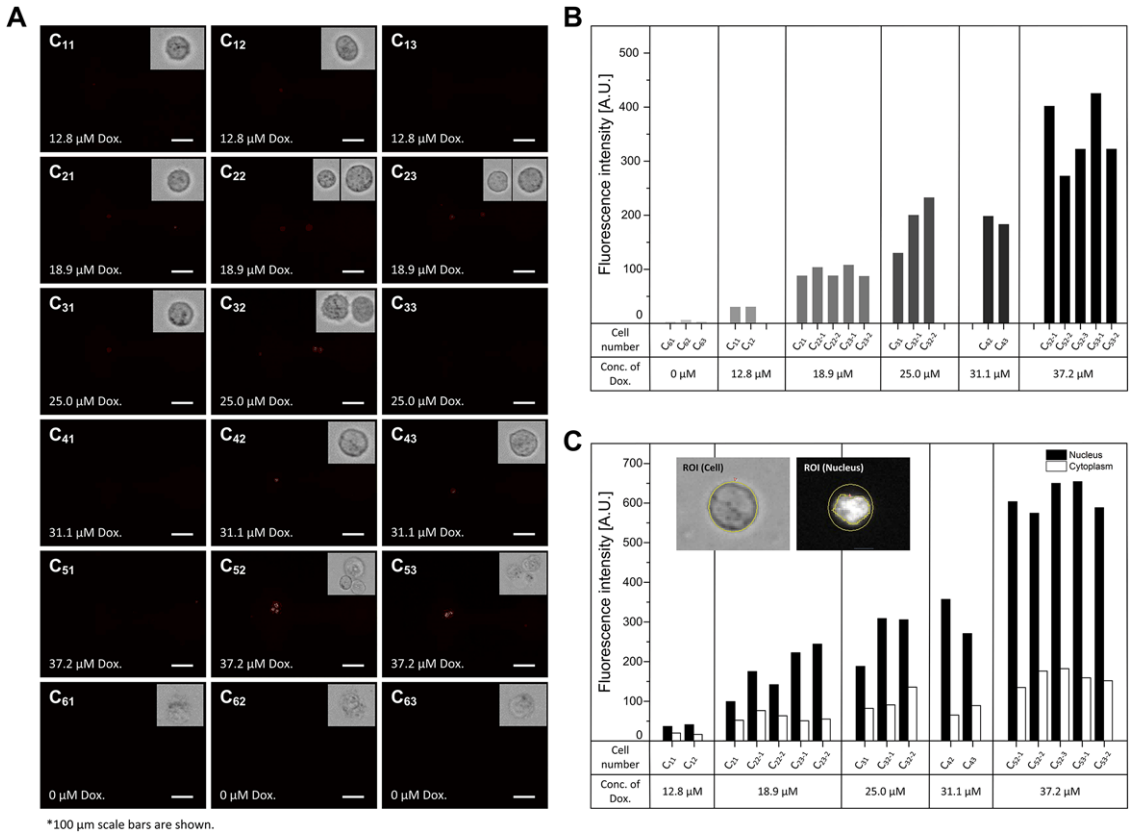

Figure 5. Doxorubicin uptake monitored at the single cell level in 18 independent chambers using a series of 6 concentrations of the drug. (A) Fluorescence microscopy images taken with a 10× magnification in the 18 chambers after exposure of the cells for 2 h to doxorubicin. In the top right corner of each chamber the bright field images of the cell(s) are shown (images not to scale). (B) Doxorubicin fluorescence intensity measured in individual cells (whole cell) in each of the 18 chambers. (C) Doxorubicin fluorescence intensity measured in the nucleus (black) and cytoplasm (white) of each cell in the 18 chambers.

This work is supported by NanoNextNL, a micro and nanotechnology consortium of the Government of the Netherlands and 130 partners.

The authors have declared no conflict of interest.

5 References

[1] McGranahan, N., Swanton, C., *Cancer Cell* 2015, *27*, 15–26.

[2] Niepel, M., Spencer, S. L., Sorger, P. K., *Curr. Opin. Chem. Biol.* 2009, *13*, 556–561.

[3] Lage, H., *Cell. Mol. Life Sciences* 2008, *65*, 3145–3167.

[4] Durand, R. E., Olive, P. L., *Cancer Res.* 1981, *41*, 3489–3494.

[5] Arora, H. C., Jensen, M. P., Yuan, Y., Wu, A., Vogt, S., Paunesku, T., Woloschak, G. E., *Cancer Res.* 2012, *72*, 769–778.

[6] Wong, H. L., Bendayan, R., Rauth, A. M., Xue, H. Y., Babakhanian, K., Wu, X. Y., *J. Pharmacol. Exp. Ther.* 2006, *317*, 1372–1381.

[7] Shen, F., Chu, S., Bence, A. K., Bailey, B., Xue, X., Erickson, P. A., Montrose, M. H., Beck, W. T., Erickson, L. C., *J. Pharmacol. Exp. Ther.* 2008, *324*, 95–102.

[8] De Lange, J., Schipper, N., Schuurhuis, G., Ten Kate, T., Van Heijningen, T. H., Pinedo, H., Lankelma, J., Baak, J., *Cytometry* 1992, *13*, 571–576.

[9] Wu, M.-H., Huang, S.-B., Lee, G.-B., *Lab Chip* 2010, *10*, 939–956.

[10] Wang, Z., Kim, M.-C., Marquez, M., Thorsen, T., *Lab Chip* 2007, *7*, 740–745.

[11] Kim, J., Taylor, D., Agrawal, N., Wang, H., Kim, H., Han, A., Rege, K., Jayaraman, A., *Lab chip* 2012, *12*, 1813–1822.

[12] Brouzes, E., Medkova, M., Savenelli, N., Marran, D., Twardowski, M., Hutchison, J. B., Rothberg, J. M., Link, D. R., Perrimon, N., Samuels, M. L., *Proc. Natll. Acad. Sci.* 2009, *106*, 14195–14200.

[13] Lee, P. J., Hung, P. J., Rao, V. M., Lee, L. P., *Biotechnol. Bioengin.* 2006, *94*, 5–14.

[14] Montanez-Sauri, S. I., Sung, K. E., Berthier, E., Beebe, D. J., *Integr. Biol.* 2013, *5*, 631–640.

[15] Bauer, M., Su, G., Beebe, D. J., Friedl, A., *Integrative Biology* 2010, *2*, 371–378.

[16] Toh, Y.-C., Lim, T. C., Tai, D., Xiao, G., van Noort, D., Yu, H., *Lab Chip* 2009, *9*, 2026–2035.

[17] Köster, S., Angile, F. E., Duan, H., Agresti, J. J., Wintner, A., Schmitz, C., Rowat, A. C., Merten, C. A., Pisignano, D., Griffiths, A. D., *Lab Chip* 2008, *8*, 1110–1115.

[18] Mazutis, L., Gilbert, J., Ung, W. L., Weitz, D. A., Griffiths, A. D., Heyman, J. A., *Nat. Protocols* 2013, *8*, 870.

[19] Joensson, H. N., Andersson Svahn, H., *Angewandte Chemie International Edition* 2012, *51*, 12176–12192.

[20] Sarkar, S., Cohen, N., Sabhachandani, P., Konry, T., *Lab Chip* 2015, *15*, 4441–4450.

[21] Li, X., Chen, Y., Li, P. C., *Lab chip* 2011, *11*, 1378–1384.

[22] Khamenehfar, A., Wan, C. P. L., Li, P. C., Letchford, K., Burt, H. M., *Analyt. Bioanal. Chem.* 2014, *406*, 7071–7083.

[23] Kellogg, R. A., Gómez-Sjöberg, R., Leyrat, A. A., Tay, S., *Nature Protocols* 2014, *9*, 1713–1726.

[24] Gómez-Sjöberg, R., Leyrat, A. A., Pirone, D. M., Chen, C. S., Quake, S. R., *Analytical Chemistry* 2007, *79*, 8557–8563.

[25] Wlodkowic, D., Faley, S., Zagnoni, M., Wikswo, J. P., Cooper, J. M., *Analytical Chemistry* 2009, *81*, 5517–5523.

[26] Torisawa, Y.-s., Mosadegh, B., Bersano-Begey, T., Steele, J. M., Luker, K. E., Luker, G. D., Takayama, S., *Integrative Biol.* 2010, *2*, 680–686.

[27] Kolnik, M., Tsimring, L. S., Hasty, J., *Lab chip* 2012, *12*, 4732–4737.

[28] Somaweera, H., Ibragimov, A., Pappas, D., *Analyst* 2013, *138*, 5566–5571.

[29] Gao, Y., Li, P., Pappas, D., *Biomedical microdevices* 2013, *15*, 907–915.

[30] Rho, H. S., Yang, Y., Hanke, A. T., Ottens, M., Terstappen, L. W., Gardeniers, H., *Lab Chip* 2016, *16*, 305–311.

[31] Unger, M. A., Chou, H.-P., Thorsen, T., Scherer, A., Quake, S. R., *Science* 2000, *288*, 113–116.

[32] Yang, Y., Swennenhuis, J. F., Rho, H. S., Le Gac, S., Terstappen, L. W., *PLoS One* 2014, *9*, e107958.

[33] Rho, H. S., Hanke, A. T., Ottens, M., Gardeniers, H., *PloS one* 2016, *11*, e0153437.

[34] Chou, H.-P., Unger, M. A., Quake, S. R., *Biomedical Microdevices* 2001, *3*, 323–330.

[35] Yang, Y., Rho, H. S., Stevens, M., Tibbe, A. G., Gardeniers, H., Terstappen, L. W., *Lab Chip* 2015, *15*, 4331–4337.

[36] Brownlee, K. A., *Statistical theory and methodology in science and engineering*, Wiley New York 1965.

[37] Keizer, H. G., Schuurhuis, G. J., Broxterman, H. J., Lankelma, J., Schoonen, W. G., van Rijn, J., Pinedo, H. M., Joenje, H., *Cancer Res.* 1989, *49*, 2988–2993.

